Do Cooperative Proton−Hydride Interactions Explain the Gas−Solid Structural Difference of BH₃NH₃?

Gabriel Merino, Vladimir I. Bakhmutov, and Alberto Vela*,[1]

Departamento de Química, Centro de Investigación y de Estudios Avanzados. A.P. 14-740, C.P. 07000, México D.F, México

The solid/gas structural differences in the weak donor−acceptor complex BH₃NH₃ is theoretically studied using density functional and the topological analysis of the electron density. The analysis shows that the cooperative dihydrogen interactions are not the main organizing factors in the molecular aggregations affecting donor−acceptor bond lengths. These aggregations are primarily controlled by electrostatic dipole−dipole interactions. This fact can be exploited in the development of simple electrostatic models that will allow the prediction of the basic structure of supramolecular architecture.

I. Introduction

The origin of the remarkable solid/gas structural differences in the weak donor−acceptor complexes has been the focus of many recent works.[2−4] Even though these structural differences are less significant in BH₃NH₃ (**1**), which has a strong B−N bond,[2c] this complex has a shorter B−N bond length in the solid (1.58 Å[3b]) than in the gas phase (1.657 Å[3c]). Hydride atoms act as proton acceptors forming nonclassic H$^{\delta+}$···$^{-\delta}$H bonds.[4] This bonding, recently reviewed,[4h] might play a primary role in molecular aggregations affecting crystal packing and supramolecular assembly.[4i] This is the case of **1** that has the proton (NH) and hydride (BH) partners, providing the motifs for self-association. For this reason, complex **1** and its dimers, have attracted the attention of chemists.[2c,3b,4a,d−f,5a] Popelier,[4f] studying one of the dimers by the topological analysis of the electron density[5b] (TAED), showed that the close H$^{\delta+}$···$^{-\delta}$H contacts can indeed be formulated as dihydrogen (DH) bonds. In this Letter we report on DFT studies of cooperative DH bonds participating in the molecular aggregation of **1** and their influence on the B−N bond length, focusing on the TAED and the electrostatic explanation for the shortening of dative bonds.

II. Results and Discussion

The optimized geometry[6] of **1** (Figure 1) agrees well with the gas-phase structure and the B−N bond length is elongated with respect to the solid state. Among the possible dimers,[2c,4a,f,5a] structures **1A** and **1B** are local minima. Two other structures, one of them with C$_{2h}$ symmetry,[2c,5a] and the other one, the dimer considered by Popelier[4f] with ΔE = 3.8 kcal/mol with respect to **1A**, are transition states. A C$_{2h}$ structure **1C**, where each
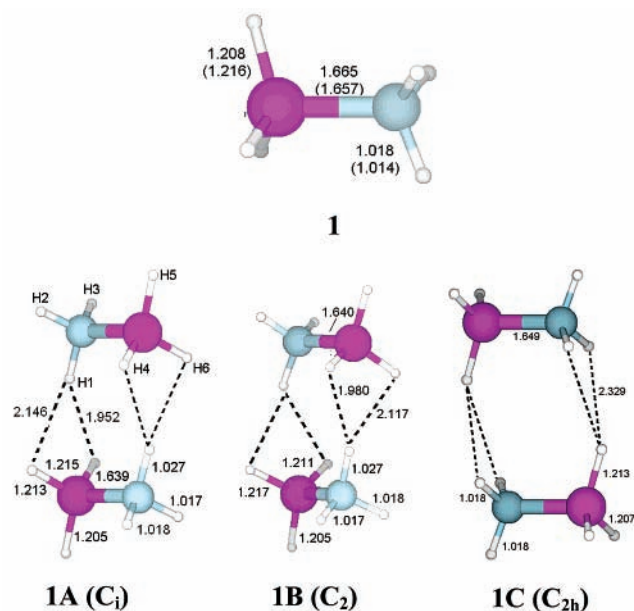

Figure 1. Structures of complex **1** and its dimers. The values in parentheses refer to the gas-phase structure of **1**. Blue spheres are nitrogen atoms and purple spheres are boron atoms.

hydride atom is directed toward two proton atoms, showed two imaginary frequencies and a ΔE = 5.3 kcal/mol. **1B** (C$_2$, ΔE = 0.3 kcal/mol) was previously reported by Crabtree et al.[4a] but structure **1A** (C$_i$) is more stable. Clearly, this diversity of stationary points and small ΔE values reflect the flatness of the potential energy surface and points toward the existence of a dynamics that interconverts the isomers. Therefore, it is

TABLE 1: Number of the Closest DH Contacts (*N*), the Electronic Density (ρ$_C$, au), and the Laplacian of the Density (∇²ρ$_C$, au) at CPs, B−N Bond Lengths (*r*(B−N), Å) in the Geometry-Optimized Complexes, Relative Energies (Δ*E*, Δ*E*$_{ZPE}$), DDI Energies for the Nonrelaxed (*E*$_{DDI}$) and Relaxed Models (*E*$_{DDI}^R$) in kcal/mol, and Dipole Moments of the Central (μ$_C$) and External (μ$_E$) Fragments (D)

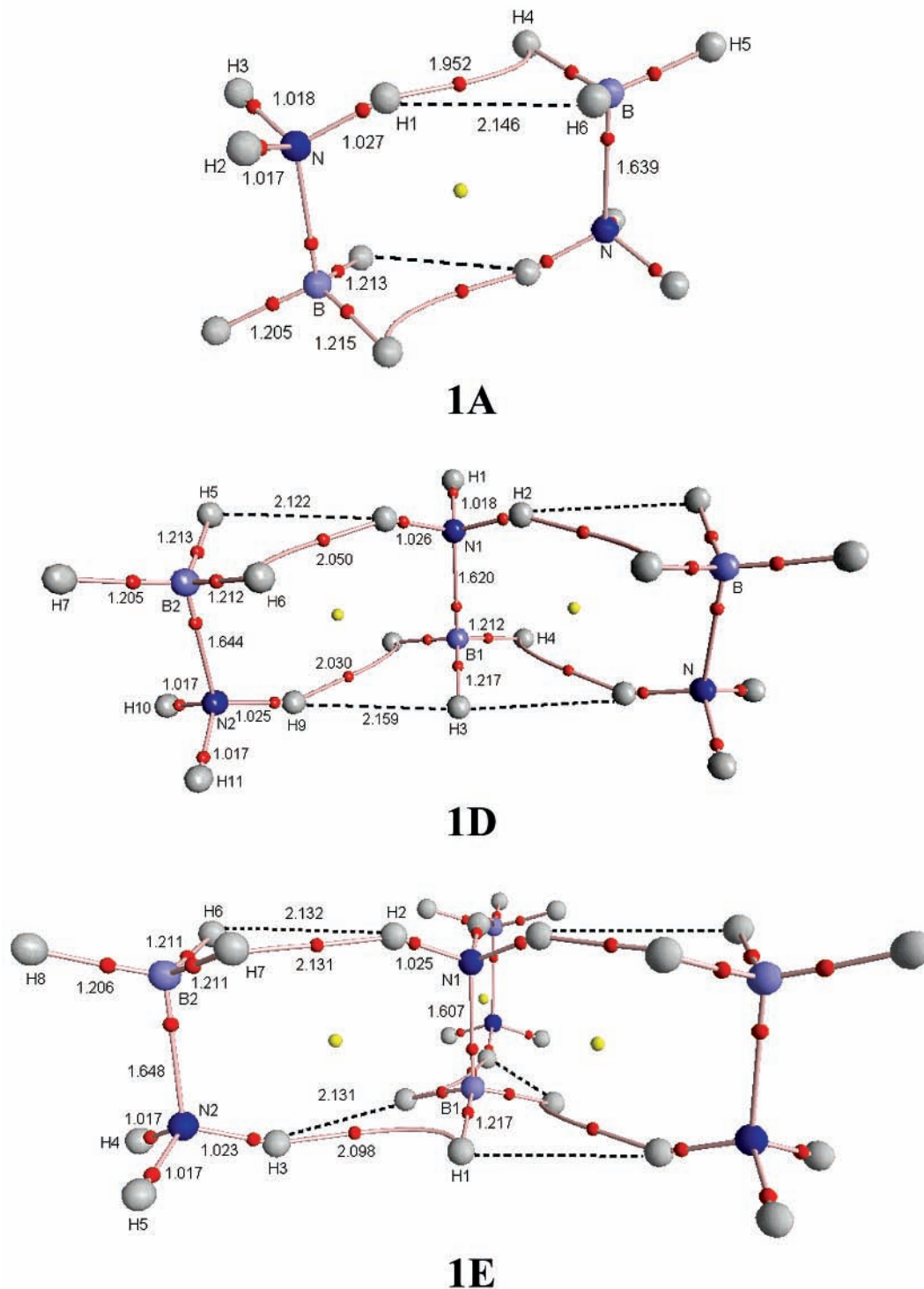| complex	*N*	ρ$_C$(H−H) (∇²ρ$_C$)	ρ$_C$(B−N) (∇²ρ$_C$)	*r*(B−N)	Δ*E* (Δ*E*$_{ZPE}$)	*E*$_{DDI}$ (*E*$_{DDI}^R$)	μ$_C$ (μ$_E$)
1	0	0 (0)	0.100 (0.406)	1.665	0 (0)		5.44
1A	2	0.016 (0.045)	0.110 (0.388)	1.639	12.8 (11.2)	11.6 (12.0)	5.54
1D	4	0.014 (0.040)	0.118 (0.370)	1.620	22.7 (19.9)	20.2 (21.3)	5.62 (5.52)
1E	6	0.012 (0.036)	0.125 (0.362)	1.607	29.7 (28.5)	25.9 (27.5)	5.68 (5.50)

Figure 2. Molecular graphs of dimer **1A**, trimer **1D**, and tetramer **1E**. Red and yellow spheres are the bond and ring critical points, respectively.

reasonable to expect that the B−N bond lengths in **1A** and **1B** should be very similar.

DH contacts in the dimers are smaller than the sum of the van der Waals radii of H (2.4 Å), suggesting an underlying stabilization mechanism driven by DH bonds. **1A**, lying in a global minimum, has two different pairs of $H^{\delta+}\cdots^{-\delta}H$ contacts. In agreement with previous theoretical studies,[8b] TAED reveals critical points (CP) only along the shorter H1···H4 directions[8a] (Figure 2). The values of the descriptors correspond to closed-shell interactions[5b] (Table 1).

It is worth noting that the densities at these CPs (ρ_C) are higher than those in weaker DH contacts like CH···HB.[4g]

Comparison of **1** and **1A** reveals that the B−H4 and N−H1 bond lengths, which take part in the DH bonding, are remarkably elongated. This effect, typical of DH bonds,[4d,e] correlates well with the electronic density at the B−H and N−H CPs: $\rho_C(B-H) = 0.168$ and $\rho_C(N-H) = 0.338$ au in **1**, versus $\rho_C(B-H4) = 0.162$ and $\rho_C(N-H1) = 0.329$ au in **1A**. The ρ_C values at the B−H5 and N−H2,3 CPs are practically invariant. The shortening of the B−N bond length in **1A** is accompanied by a corresponding increase in its ρ_C (Table 1). In contrast to **1A**, dimer **1C** with the longest $H^{\delta+}\cdots^{-\delta}H$ contacts has the longest N−B bond length, which is closer to the monomer.

Letters

J. Phys. Chem. A, Vol. 106, No. 37, 2002 **8493**

A shorter B−N bond length is observed in the central fragment of trimer **1D** (Figure 2). The side molecules have longer B−N distances (ρ_C(B2−N2) = 0.108 au) than in **1A**. TAED reveals four CPs only in the shortest $H^{\delta+}\cdots^{-\delta}H$ contacts, which become longer than in **1A** and have a smaller ρ_C (Table 1). All the tendencies are more pronounced in tetramer **1E**: the B−N bond length in the central fragment, surrounded by three BH_3NH_3 molecules, is smaller, and again, the $H^{\delta+}\cdots^{-\delta}H$ distances increase. Six of them show CPs. Note that classical H-bonds, C−H···N, for example, get shorter as the molecular aggregation increases.[9a] Finally, the closest $H^{\delta+}\cdots^{-\delta}H$ contacts in the dimer, trimer, and tetramer are very similar to those found in the neutron diffraction structure of **1** (2.02(3) Å).[3b]

The B−N shortening from **1A** to **1E** is accompanied by the appearance of a network of DH gradient paths. Richardson et al.[4a] have proposed that the total association energy of these systems is due to the presence of DH contacts. This suggestion can be supported by the TAED depicted in **1A**−**E**. Using the association energies reported in Table 1, and following the later model, one finds that the energy of each DH contact decreases on going from the dimer to the tetramer (6.4 (**1A**) > 5.7 (**1D**) > 4.95 (**1E**) kcal/mol). Thus, because these energies are becoming weaker, one cannot support that the cooperativity of the DH contacts is the main factor driving the aggregation of these systems. An alternative to rationalize this effect is to note that the central fragment in **1D,E** is surrounded by dipoles (external fragments), all of them oriented in the same direction and opposite to the direction of the central fragment, which induce an electric field in the central moiety that "pushes" the electron pair of N toward B and, thus, strengthens the B−N bond.[8b,10] This displacement of the lone pair is accompanied by a change in the local geometry of the BH_3 fragment, which approaches an almost tetrahedral coordination in the tetramer (the N−B−H angle goes from ∼105° in the monomer, to 108.4° in the tetramer). However, the NH_3 fragment remains almost unchanged (see Table 6-SM, Supporting Information). The strengthening of the B−N bond is further supported by the fact that ρ_C increases and $\nabla^2\rho_C$ decreases at the B−N critical points. Previous works have addressed this issue and have suggested that the electrostatic interaction, mainly the dipole−dipole, is primarily responsible for the association.[2b,c,3a] However, none of these works provided an estimation of the contribution of the electrostatic forces to the association energy. In this vein, here we propose a simple electrostatic model that produces the dipole−dipole interaction (DDI) energies reported in Table 1.[11] Comparison of the ΔE and E_{DDI} values shows that the aggregation driving force is mainly the electrostatic DDI, in agreement with the suggestions of previous works. If one assumes that the total interaction energy, ΔE, has an electrostatic dipole−dipole term, E_{DDI}^R, and a contribution due to the DH contacts, then the latter contributions are 0.8, 1.4, and 2.2 kcal/mol in **1A**, **1D**, and **1E**, respectively. These values correlate almost linearly with the number of existing CPs between protons and hydrides and provide a 0.4 kcal/mol estimation for the energy of each DH contact, which is 1 order of magnitude smaller that the value reported by Richardson et al.[4a]

III. Conclusions

In conclusion, the analysis presented herein shows that the cooperative dihydrogen interactions are not the main organizing factors in the molecular aggregations affecting the bond shortening of the donor−acceptor BH_3NH_3 system. A very simple electrostatic model shows that these aggregations are primarily controlled by dipole−dipole interactions, supporting the suggestions and observations of previous authors. Preliminary calculations indicate that this explanation can be extended to other donor−acceptor systems. This fact can be exploited in the development of simple electrostatic models that will allow the prediction of the basic structure of supramolecular architecture.

Supporting Information Available: Complete optimized geometries, total energies, zero-point corrections, dipole moments and bond descriptors of **1** and **1A**−**E**. This material is available free of charge via the Internet at http://pubs.acs.org.

References and Notes

(1) E-mail: avela@mail.cinvestav.mx.

(2) (a) Buhl, M.; Steinke, T.; Schleyer, P.; Boese, R. *Angew. Chem., Int. Ed. Engl.* **1991**, *30*, 1160. (b) Leopold, K. R.; Burns, W. A. *J. Am. Chem. Soc.* **1993**, *115*, 11622. (c) Jonas, V.; Frenking, G.; Reetz, M. T. *J. Am. Chem. Soc.* **1994**, *116*, 8741.

(3) (a) Leopold, K. R.; Canagaratna, M.; Phillips, J. A. *Acc. Chem. Res.* **1997**, *30*, 57. (b) Klooster, W. T.; Koetzle, T. F.; Siegbahn, P. E. M.; Richardson, T. B.; Crabtree, R. H. *J. Am. Chem. Soc.* **1999**, *121*, 6337. (c) Thorne, L. R.; Suenram, R. D.; Lovas, F. J. *J. Chem. Phys.* **1983**, *78*, 167.

(4) (a) Richardson, T. B.; de Gala, S.; Crabtree, R. H.; Siegbahn, P. E. M. *J. Am. Chem. Soc.* **1995**, *117*, 12875. (b) Shubina, E. S.; Belkova, N. V.; Krylov, A. N.; Vorontsov, E. V.; Epstein, L. M.; Gusev, D. G.; Niedermann, M.; Berke, H. *J. Am. Chem. Soc.* **1996**, *118*, 1105. (c) Peris, E.; Wessel, J.; Patel, B. P.; Crabtree, R. H. *J. Chem Soc., Chem. Commun.* **1995**, 2175. (d) Bakhmutova, E. V. Ph.D. Thesis, Moscow, 2000. (e) Epstein, L. M.; Shubina, E. S.; Bakhmutova, E. V.; Saitkulova, L. N.; Bakhmutov, V. I.; Chistyakov, A. L.; Stankevich, I. V. *Inorg. Chem.* **1998**, *37*, 3013. (f) Popelier, P. L. A. *J. Phys. Chem. A* **1998**, *102*, 1873. (g) Güizado-Rodríguez, M.; Ariza-Castolo, A.; Merino, G.; Vela, A.; Noth, H.; Bakhmutov, V. I.; Contreras, R. *J. Am. Chem. Soc.* **2001**, *123*, 9144. (h) Custelcean, R.; Jackson, J. E. *Chem. Rev.* **2001**, *101*, 1963. (i) Yokoyama, T.; Yokoyama, S.; Kamikado, T.; Okuno, Y.; Mashiko, S. *Nature* **2001**, *413*, 619.

(5) (a) Cramer, C. J.; Gladfelter, W. L. *Inorg. Chem.* **1997**, *36*, 5358. (b) Bader, R. F. W. *Atoms in Molecules. A Quantum Theory*; Oxford University Press: NY, 1990.

(6) Geometry optimizations of the molecules were performed with Gaussian[7] using the B3LYP functional and with a 6-311++G(d,p) basis set. Every stationary point was characterized by a harmonic analysis. TAED was done with the density matrix obtained from the Gaussian calculation of each structure that was fed to Bader's AIMPAC program package. Cartesian coordinates, total energies, zero point energy corrections, dipole moments and the descriptors of some of the critical points corresponding to structures **1**, **1A**, **1D**, and **1E**, can be found in Tables 1-SM to 4-SM (Supporting Information), respectively. From the total energies and zero point energy (ZPE) corrections, the relative energies (ΔE and ΔE_{ZPE}) of the structures were obtained. To validate the selection of exchange-correlation energy functional and basis set, calculations for the monomer and the dimer with LDA, BLYP, and B3LYP were performed. For each of these functionals the following basis sets were analyzed: DZVP2, TZVP, and 6-311++G(d,p). From a comparison of the gas-phase structure[3c] and MP2[5a] calculations with large basis sets, one concludes that the B3LYP functional with a 6-311++G(d,p) basis set is the best theoretical methodology to study this system. See Table 5-SM in the Supporting Information. The molecular graphs were done with AIM2000 (Version 1.0) (F. Biegler-Köning, University of Applied Sciences, Bielefeld, Germany, 2000).

(7) Frisch, M. J.; Trucks, G. W.; Schlegel, H. B.; Scuseria, G. E.; Robb, M. A.; Cheeseman, J. R.; Zakrzewski, V. G.; Montgomery, J. A.; Stratmann, R. E.; Burant, J. C.; Dapprich, S.; Millam, J. M.; Daniels, A. D.; Kudin, K. N.; Strain, M. C.; Farkas, O.; Tomasi, J.; Barone, V.; Cossi, M.; Cammi, R.; Mennucci, B.; Pomelli, C.; Adamo, C.; Clifford, S.; Ochterski, J.; Petersson, G. A.; Ayala, P. Y.; Cui, Q.; Morokuma, K.; Malick, D. K.; Rabuck, A. D.; Raghavachari, K.; Foresman, J. B.; Cioslowski, J.; Ortiz, J. V.; Stefanov, B. B.; Liu, G.; Liashenko, A.; Piskorz, P.; Komaromi, I.; Gomperts, R.; Martin, R. L.; Fox, D. J.; Keith, T.; Al-Laham, M. A.; Peng, C. Y.; Nanayakkara, A.; Gonzalez, C.; Challacombe, M.; Gill, P. M. W.; Johnson, B. G.; Chen, W.; Wong, M. W.; Andres, J. L.; Head-Gordon, M.; Replogle, E. S.; Pople, J. A. *Gaussian 98*, Revision A.7; Gaussian, Inc.: Pittsburgh, PA, 1998.

(8) (a) The ρ values in bond B−H6, directed to H1, is reduced (0.162 au) with respect to trans-oriented bond B−H5 or bonds B−H in **1** (ρ_C(B−H) = 0.167 au). Therefore, even small molecular deformations can result in the appearance of the CPs along directions H1···H6 and hence the DH bonds have a proclivity to bifurcate. (b) Kulkarni, S. A.; Srivastava, A. K. *J. Phys. Chem. A* **1999**, *103*, 2836.

(9) (a) Karphen, A. *J. Phys. Chem*. **1996**, *100*, 13475. (b) Rasul, G.; Surya Prakash, G. K.; Olah, G. A. *Inorg. Chem*. **1999**, *38*, 44.

(10) Raymo, F. M.; Bartberger, M. D.; Houk, K. N.; Stoddart, J. F. *J. Am. Chem. Soc*. **2001**, *123*, 9264.

(11) Dipole moments oriented along the B−N bonds and centered at the midpoints of these bonds were used to evaluate the classical DDI. In the nonrelaxed model, the dipole moment of each interacting fragment in the complexes is equal to that of the free monomer. As it is explained in the main text, the shortening of the central B−N bond length induces a relaxation on the dipole moments of the fragments. To take into account this relaxation, the dipole moments of each fragment in each complex were calculated using the optimized geometry of the fragment in the corresponding complex and the DDI energy was calculated with these dipole moments. This corresponds to the relaxed model.